Apoptotic and autophagic cell death induced in cervical cancer cells by a dual specific oncolytic adenovirus

Shanzhi Li[a], Zhuoxin Li[a], Shuang Chen[b], Yilong Zhu[a], Yiquan Li[a], Xunzhe Yin[c], Xiao Li[a,b] and Guangze Zhu[a]

Objective **Oncolytic adenoviruses are capable of exerting anticancer effects via a variety of mechanisms, including apoptosis and autophagy. In the present study, the dual-specific antitumor oncolytic adenovirus, Ad-Apoptin-hTERT-E1a (ATV), was used to infect cervical cancer cell lines to test its antitumor effects.**

Methods **To explore the use of apoptin in tumor gene therapy, a recombinant adenovirus ATV expressing the apoptin protein was assessed to determine its lethal and growth-inhibitory effects on human cervical cancer cell line (HeLa) cells *in vitro*. Nonapoptotic autophagy of HeLa cells infected with ATV was assessed by examining the cell morphology, development of acidic vesicular organelles and the conversion of microtubule-associated protein 1 light chain 3 (LC3) from its cytoplasmic to autophagosomal membrane form. Using gene silencing (knockdown of LC3 and Belin-1), autophagy-associated molecules (e.g. ATG5, ATG12 and ULK1) were monitored by real-time PCR and western blot.**

Results **A series of experiments demonstrated that ATV could significantly induce apoptosis and autophagy in cervical cancer cells, and provided evidence that ATV not only induced apoptosis but also autophagy and ATG5, ATG12 and ULK1 related pathways were not entirely dependent on LC3 and Beclin-1.**

Conclusion **These results indicate that ATV may have a potential application in tumor gene therapy. *Anti-Cancer Drugs* 34: 361–372 Copyright © 2022 The Author(s). Published by Wolters Kluwer Health, Inc.**

Anti-Cancer Drugs 2023, **34**:361–372

Keywords: apoptosis, autophagy, cervical cancer HeLa cell lines, oncolytic adenovirus, RNAi

[a]Changchun University of Chinese Medicine, [b]Changchun Veterinary Research Institute, Chinese Academy of Agricultural Sciences and [c]Changchun Institute of Applied Chemistry, Chinese Academy of Sciences, Changchun, People's Republic of China

Correspondence to Xunzhe Yin, PhD, Changchun Institute of Applied Chemistry, Chinese Academy of Sciences, No. 5625, Renmin Street, Changchun, Jilin province, 130022, People's Republic of China
E-mail: xzyin@ciac.ac.cn

Received 27 September 2022 **Revised form accepted** 29 September 2022.

Introduction

Cervical cancer is the third most common cancer among female-specific malignant tumors with an estimated 600 000 cases and 300 000 deaths in 2021 worldwide according to the latest global cancer statistics report of 2021. In addition, this disease ranks as the fourth most frequently diagnosed cancer and the fourth leading cause of cancer death and the age of onset is gradually decreasing [1]. Among these cervical cancer patients, approximately 95% of cases are caused by persistent infections with high risk human papillomavirus. In addition, the morbidity and mortality of cervical cancer account for a high proportion of cases, and cervical squamous cell carcinoma is the most susceptible pathological type of cervical cancer [2,3]. Therefore, a precise understanding of the complex cellular/molecular mechanisms underlying the initiation, progression, and prevention of the uterine cervix is essential. It is important to note that cervical cancer treatment advocates early prevention, detection and treatment.

Oncolytic viruses comprise an emerging cancer therapeutic modality whose activity involves both direct tumor cell lysis and the induction of immunogenic cell death [4] and includes different types of oncolytic viruses (e.g. adenoviruses, alphaviruses, herpes simplex viruses, Newcastle disease viruses, rhabdoviruses and coxsackie viruses) [5]. Gene therapy offers a promising strategy for patients who are resistant to traditional therapies due to its advantage of selectively correcting or eradicating defective tissues and targeting defects in malignant cells [6]. An increasing number of clinical trials involving oncolytic adenoviruses have been conducted over the past two decades [7]. The tumor selectivity of oncolytic viruses is largely conferred by tumor-specific aberrations in signaling pathways that normally sense and block viral replication. Therefore, cells that become malignant by evolving defects in interferon signaling often unwittingly become sensitive to viral infection. Therefore, the modulation of apoptosis through targeting pro-apoptotic and antiapoptotic proteins may be a powerful and effective method for treating cancer. Furthermore, apoptin, a protein derived from the

This is an open-access article distributed under the terms of the Creative Commons Attribution-Non Commercial-No Derivatives License 4.0 (CCBY-NC-ND), where it is permissible to download and share the work provided it is properly cited. The work cannot be changed in any way or used commercially without permission from the journal.

chicken anemia virus, has received significant attention as a selective killer of cancer cells.

Therefore, we sought to identify new substances with high antiproliferative activity but low necrotic effects capable of inducing apoptosis and autophagy. Apoptosis plays a key role in the mechanism of innate inhibition of cancer; thus, its occurrence is also related to the imbalance of apoptosis in cancer cells. Apoptin not only induces monocyte apoptosis but also has the ability to specifically recognize and replicate in tumor cells. The released progeny viral particles can diffuse into tumor cells and directly lyse human tumors (e.g. hepatocellular carcinoma, melanoma, breast cancer, lung cancer and colon cancer). In contrast, apoptin has no effect on fibroblasts, skin cells or smooth muscle cells. In addition, autophagy is emerging as an important biological mechanism for targeting human cancers, including cervical cancer. Furthermore, autophagy, a process of cytoplasmic and cellular organelle degradation in lysosomes has been implicated in homeostasis. Additionally, autophagic flux may vary depending on the cell and tissue type, thereby altering the cellular fate under conditions of stress leading to cell survival and death. Autophagy may in turn govern tumor metastasis and subsequent carcinogenesis. Thus, the targeted manipulation of complex autophagic signaling may prove to be an innovative strategy in the identification of clinically relevant biomarkers associated with cervical cancer in the near future [8].

The present study aimed to determine whether the recombinant adenovirus, Ad-Apoptin-hTERT-E1a (ATV), was able to target human cervical cancer cell line (HeLa) cell apoptosis and induce autophagy *in vitro*, as well as elucidate the underlying mechanism. The results of our study were verified and provided a novel strategy for gene therapy research in cervical cancer.

Materials and methods

Roswell park memorial institute (RPMI)-1640 medium and fetal bovine serum (FBS) were purchased from Hyclone, USA. Rabbit antibodies against LC3B (CST, #3868, USA) and Beclin-1 (CST, #3495, USA) were purchased from Cell Signaling Technology. Horseradish peroxidase (HRP)-conjugated anti-rabbit, IgG antibodies were purchased from ZSGB-Bio (China). A halt protease inhibitor cocktail, immunol precipitation (IP) Lysis buffer, and bicinchoninic acid (BCA) kit (Beyotime, P0012, China) for a protein assay were procured from Beyotime. Pierce enhanced chemiluminescence (ECL) western blotting Substrate and Lipofectamine 2000 were purchased from Thermo Fisher Scientific. Fluorescent antibody (FITC) Annexin V Apoptosis Detection I (BD, 556547, USA) and propidium iodide/RNase Staining Butter (BD, 550825, USA) were purchased from BD Pharmingen. Cell Proliferation Reagent was procured from Roche (USA). Monodansylcadaverin was purchased from Sigma (Sigma-Aldrich, 30432, Germany); UNlQ-10 Column Trizol Total RNA Isolation Kit (Sangon, B511321, China) was purchased from Sangon Biotech.

Cell culture

The oncolytic adenovirus and HeLa cell lines were obtained from the Changchun Veterinary Research Institute. HeLa cells were cultured in RPMI-1640 medium supplemented with 10% (v/v) FBS (Hyclone, USA), and 1% penicillin-streptomycin (Hyclone, USA). Cultures were maintained in a humidified atmosphere with 5% CO_2 at 37 °C. All cell-based assays were performed using cells in the exponential growth phase.

Cell proliferation assays

Assays were performed by seeding 5000 cells in the exponential growth phase per well in 96-well tissue culture plates at a volume of 100 µL RPMI-1640 medium at 37 °C in 5% CO_2. After 24 h, the HeLa cells were infected with 100 multiplicity of infection (MOI) of ATV, with Ad-oncolytic adenovirus empty vector (MOCK) used as the control group (three wells/group). After culturing for 6, 12, 24, 48 and 72 h, water soluble tetrazolium salt (WST)-1 was added to each well, cultured at 37 °C and 5% CO_2 and were incubated for 90 min, as well as in the control group. The absorbance (A) was measured at a wavelength of 490 nm and the cellular proliferation inhibition rate was calculated according to the formula: the cell proliferation inhibition rate = (A of control group − A of the treated group)/A of control group × 100%.

Annexin V assay

HeLa cells were seeded at a density of 200 000 cells/well in a six-well plate and cultured for 24 h in a humidified atmosphere containing 5% CO2 at 37 °C. HeLa cells were infected with 100 MOI of ATV for 24, 48 and 72 h, with Ad-MOCK as the control group. An Annexin-V assay was conducted following the manufacturer's instructions. The cell suspension was mixed with 5 µL Annexin-V-FITC and 5 µL propidium iodide (50 mg/mL) for 15 min. The apoptotic rate was analyzed using a fluorescence activated cell sorting Calibur flow cytometer (Becton Dickinson, USA). Annexin V-FITC binding was detected by flow cytometry acquiring a minimum of 20 000 events from each sample. An apoptotic data analysis was performed using CellQuest software (Becton Dickinson, USA).

Cell cycle distribution analysis

As described above, after treatment, the treated cells were washed with PBS (pH 7.4) before being fixed in 75% ethanol overnight at 4 °C. Subsequently, the cells were centrifuged and the residual alcohol was aspirated, washed in PBS and stained, resuspended cells in propidium iodide/RNase staining solution and incubated at room temperature in the dark for 30 min. Finally, the samples were analyzed by flow cytometry by evaluating 20 000 events per sample and data analyses were performed using CellQuest software (Becton Dickinson, USA).

Western blot analysis

Following treatment, cells were lysed using IP Lysis buffer on ice for 30 min. The protein concentration was measured using the BCA kit and total protein (100 μg) was mixed with Lysis buffer supplemented with 5% β-mercaptoethanol and heated to 95 °C for 10 min followed by a 10 min incubation on ice. The sample was loaded in 10% SDS-PAGE and subsequently electro-transferred to a polyvinylidene difluoride membrane (PVDF). The membrane was blocked for 3 h in a 5% nonfat dry milk buffer. After blocking, the membrane was incubated with anti-glyceraldehyde-3-phosphate dehydrogenase (GAPDH) (CST, #5174, USA), anti-LC3B, anti-Beclin-1, anti-p62 (CST, #39749, USA), anti-mammalian target of rapamycin (mTOR) (CST, #2983, USA), anti-ATG12 (CST, # 4180, USA), anti-ATG5 (CST, # 12994, USA) and anti-ULK1 (CST, # 6439, USA) antibodies at 1:1000 for overnight at 4 °C. After washing, the membrane was incubated with the second HRP-conjugated secondary antibody at 1:1000 at room temperature for 2 h. The blot signals were visualized using the ECL western blotting substrate (Millipore, WBKLS0100, Germany). Gray value analysis was using ImageJ software (USA).

RNA extraction, cDNA synthesis, and quantitative real-time PCR analysis

To extract the total RNA from oncolytic adenovirus-treated HeLa cells, an UNlQ-10 Column Trizol Total RNA Isolation Kit was used, following the manufacturer's instructions as described below. The concentration was determined using a nanoparticle Drop and quantified by the minimum RNA mass. Total RNA was reverse transcribed to generate cDNA by incubating the reaction mixture (50 μL) at 42°C for 50 min containing Moloney murine leukemia virus (M-MLV) reverse transcriptase and random primer 9. Real-time quantitative real-time (qPCR) was executed in a 20 μl final volume for each primer (described below) using the SYBRGoTaq qPCR Master Mix (Promega, A6010, USA), and detected by an ABI 7000 sequence detection system. The primer sequences for LC3, Beclin-1, ATG5, ATG12, ULK1, and GAPDH (the housekeeping gene and internal control) were as follows: GAPDH (5′-GTCGGTGTGAACGGATTT-3′, 5′-ACTCCACGACGTACTCAGC-3′); LC3 (5′-AATAGAAGGCGCTTACAG-3′, 5′-GACAATTTCATCCCGAAC-3′); Beclin-1 (5′-CCGTGGTAACCTTGTTCATCC-3′, 5′-GCTCTGTCTTCAGCGACTTCC-3′); ATG5 (5′-CATACTATTTGCTTTTGCC-3′, 5′-ATTTCAGTGGTGTGCCTTC-3′); ATG12 (5′-AGTAGAGCGAACACGAACC-3′, 5′-CTGCCAAAACACTCATAGA-3′); and ULK1 (5′-CCCGCACCAGGATGTTCTCA-3′, 5′-CCCTCCAGGTTCGCAGCAAT-3′). The PCR program is designed including 95 °C for 15 s, 60 °C for 30 s, 72°C for 30 s, 40 cycles, and 72 °C for 10 min. The relative cDNA expression for each sample was computerized using the formula $2^{-\Delta\Delta Ct}$, where $\Delta\Delta Ct = \Delta Ct$ (target gene) – ΔCt (GAPDH gene), which represented the target cDNA expression normalized to GAPDH cDNA levels.

Hoechst staining analysis

The slides were placed in six-well plates to prepare HeLa cell monolayers, with a cell density of 2.0×10^5 cells/well. Cultured for 24 h and HeLa cells were infected with 100 MOI of Ad-MOCK and ATV for 12, 24, 48 and 72 h. After the time of arrival, the culture medium was discarded and washed twice with PBS. Hoechst 33342 (1:1000 dilution, Thermo Fisher, H1399, USA) was added to 1 ml and incubated in the dark for 10 min, at 37 °C in a 5% CO_2 incubator. The working solution was discarded, washed twice with PBS, and serum-free and antibiotic-free RPMI-1640 was added. The cells were observed using a fluorescence microscope (excitation filter wavelength at 355 nm and block filter wavelength at 512 nm) and photographed.

JC-1 staining detection

Glass slides and cell density were the same as those mentioned above and treated with 100 MOI Ad-MOCK and ATV for 12, 24, 48 and 72 h. The concentration of JC-1 (1:1000 dilution) was 5 μg/ml, and 1 ml was added to each well in a six-well plate incubated in the dark for 15 min, washed twice with PBS, and observed under a fluorescence microscope.

Detection of autophagy by monodansylcadaverine staining

HeLa cells were seeded at a density of 200 000 cells/well in a six-well plate and cultured for 24 h in a humidified atmosphere of 5% CO_2 at 37 °C. HeLa cells were infected with 100 MOI ATV for 6, 12, 24 and 48 h. Ad-MOCK was used as the control group. Following treatment, the cells were washed twice in PBS, 750 μl of a monodansylcadaverine staining solution (50 μmol/L) was added to a six-well plate, incubated at 37 °C in 5% CO_2 in the dark for 15 min. The cells were washed twice in PBS, then serum-free and nonantibiotic RPMI-1640 medium was added. Subsequently, the accumulation of autophagosome puncta was captured using a fluorescence microscope (Olympus, Japan).

GFP-LC3 transient transfection

For transfection, the cells were trypsinized and seeded into a six-well plate at a density of 2×10^5 cells/well. The cells were infected with 100 MOI Ad-MOCK and ATV for 12 h. Before the transfection, we first balanced the X-treme GENE HP transfection reagent, plasmid DNA (GFP-LC3 plasmid), and Opti-MEM medium for 15 min at room temperature. GFP-LC3 (3 μg) plasmids were introduced to the plates into the cells using the X-treme GENE HP transfection reagent (Roche, Switzerland) according to the manufacturer's recommendations. Cells with green spots were scored under a fluorescence microscope when the expression vector was transfected for 12 h.

Fig. 1

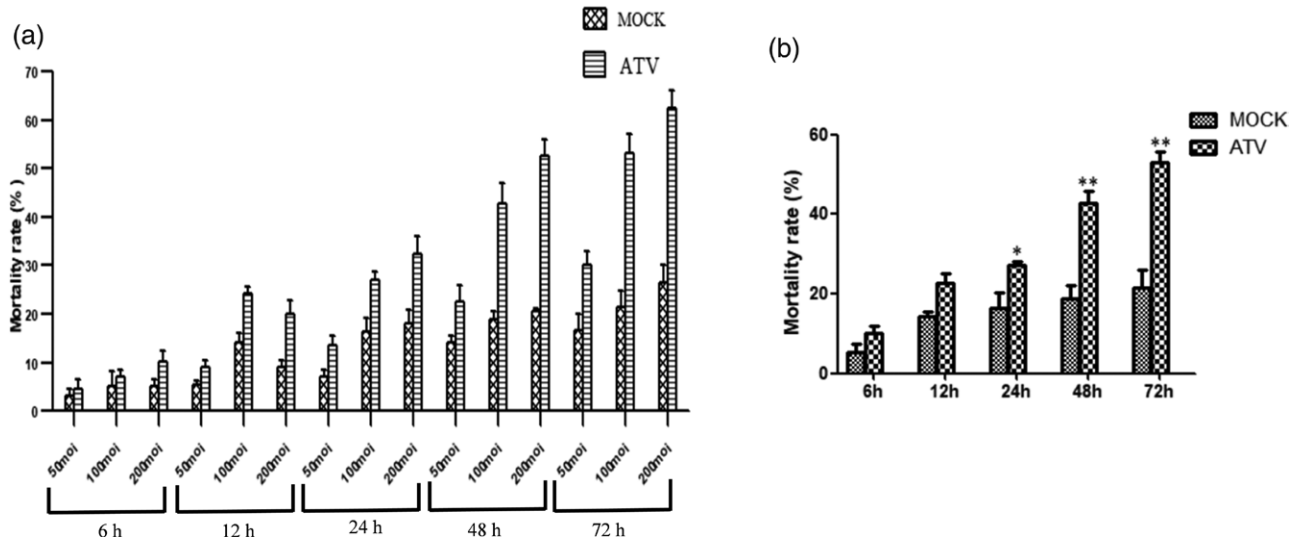

Inhibitory effects of ATV on the cell viability of human cervical cancer HeLa cell lines. Cells were treated with a variety of dosages (50 MOI, 100 MOI, and 200 MOI) of ATV for 6, 12, 24, 48 and 72 h (a) and independently with 100 MOI for 6–72 h period (b). Cellular survival was determined using a WST-1 assay. All of the data resulted from repeating independent experiments three times and the results are expressed as the mean ± SE. Values were considered to be statistically significant (Ad-MOCK treatment) for * $P<0.05$ and ** $P<0.01$ compared with the control group. HeLa, human cervical cancer cell line; MOI, multiplicity of infection; MOCK, Oncolytic adenovirus empty vector; MOI, multiplicity of infection; WST, water soluble tetrazolium salt.

Indirect immunofluorescence staining analysis

HeLa cells were grown to approximately 70% confluence on a coverslip, then treated with 100 MOI Ad-MOCK and ATV for 8 and 24 h. The culture medium was discarded and washed twice with PBS and fixed in 4% paraformaldehyde for 30 min at room temperature. Triton X-100 had permeation treatment for 10 min at room temperature, blocked in 10% bovine albumin for 2 h, and the fixed cells were stained with a fluorescently labeled anti-LC3 antibody overnight at 4 °C. 4',6-diamidino-2-phenylindole was then added to the cells in the dark, incubated for 15 min, observed, and photographed using a microscope.

Transfection of synthetic small interfering RNA

Small-interfering RNA (siRNA) against LC3 and Beclin-1, and nonspecific scrambled siRNA were synthesized by RiboBio, China. HeLa cells were cultured in six-well plates. Lipofectamine 2000 (Thermo, #11668019, USA) was mixed into Opti-MEM containing siRNA (LC3, CTAGATAGTTACACACATA), siRNA (Beclin-1, GGTCTAAGACGTCCAACAA) or scrambled RNA. Additionally, mock controls were transfected with Lipofectamine 2000 alone, incubated at room temperature for 15 min, and distributed into duplicate wells. Transfections were performed at 37 °C in 5% CO_2. After 48 h, the cells were treated with Ad-MOCK and ATV for 6, 12, 24, 48 and 72 h. The RNA was then extracted, cDNA synthesized, and quantitative real-time PCR was performed.

Statistical analysis

The statistical significance of differences was assessed using a one-way analysis of variance, in which $P<0.05$ or $P<0.01$ was considered to indicate a statistically significant difference. All statistical tests were performed using GraphPad Prism 5.0 software (GraphPad, USA).

Results

ATV inhibits the growth of human cervical cancer cells

The inhibitory effect of ATV on cervical cancer cells was investigated using a WST-1 assay. During the early stages of infection, treatment with ATV did not cause significant inhibition of the HeLa cells compared with the Ad-MOCK group. To elucidate the mechanisms underlying ATV-induced growth inhibition, we performed a WST-1 assay on cervical cancer cells treated with ATV at serial time points (6, 12, 24, 48 and 72 h). ATV significantly inhibited the growth of HeLa cells and decreased the cellular proliferation in HeLa cells in both a time- and dose-dependent manner. The inhibition rate was 200 MOI >100 MOI >50 MOI for the same infection time (Fig. 1a). The inhibitory rates of 100 MOI ATV in HeLa cells were (10.235 ± 2.270), (22.710 ± 3.535), (27.154 ± 1.487), (42.904 ± 3.969) and (53.053 ± 3.938)% at 6, 12, 24, 48 and 72 h (Fig. 1b), respectively, which was significantly higher than the Ad-MOCK group at 48 h [(42.904 ± 3.969) vs. (18.338 ± 1.1334)%; $P<0.01$]. The data indicated that the apoptin-constructed oncolytic adenovirus, ATV, can inhibit the proliferation of HeLa cells.

Annexin V detects the apoptosis rate of HeLa cells

Annexin V labeled with FITC binds to the membrane of early apoptotic cells through phosphatidylserine. Propidium iodide vs. ide is a nucleic acid dye that

Fig. 2

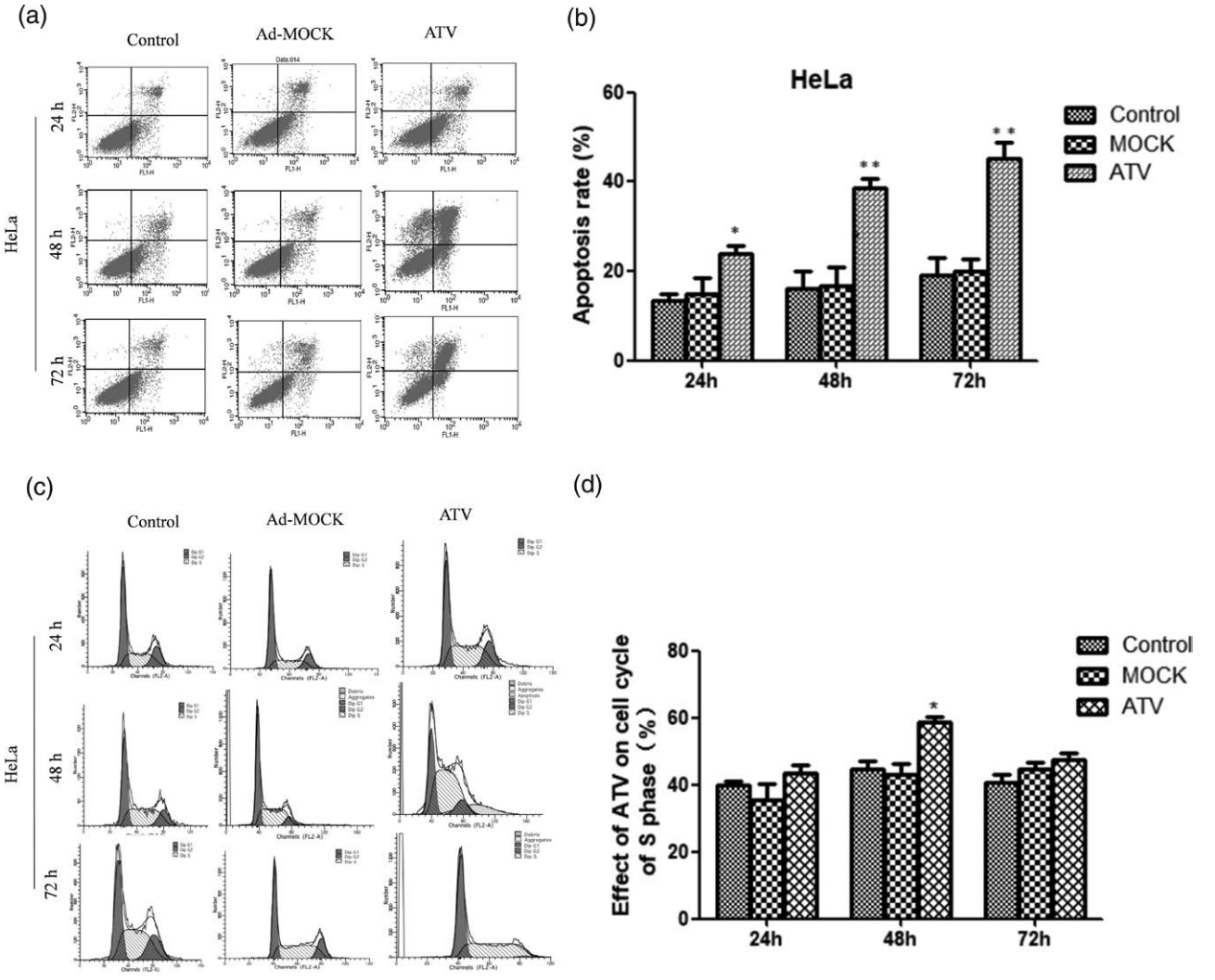

Apoptin-constructed oncolytic adenovirus ATV induces apoptosis and arrests cell cycle changes in human cervical cancer HeLa cells. ATV promoted apoptosis in human cervical cancer HeLa cells (a). The cells (2×10^4) were treated with 100 MOI ATV for 24, 48 and 72 h (b). Flow cytometric analysis of the apoptotic cell ratios following Annexin V-FITC/PI staining. Results are expressed as the means ± *SE*, ** $P<0.01$ compared with the Ad-MOCK group.HeLa cells were treated with 100 MOI ATV for 24, 48 and 72 h. The cell distribution at the G1, S, and G2/M phases was determined using flow cytometry (c). A histogram of the proportion of cells in the S phase of the cell cycle (d). All of the data resulted from repeating independent experiments and the results are expressed as the mean ± *SE*. * Values were statistically significant (versus Ad-MOCK treatment) for $P<0.05$ as compared with the control group. FITC, fluorescent antibody; MOCK, oncolytic adenovirus empty vector; MOI, multiplicity of infection.

allows cells to pass through the cell membrane to stain the nucleus during the middle and late stages of apoptosis. Staining the cells with Annexin V combined with propidium iodide was used to distinguish the cells in different stages of apoptosis. The flow cytometry results showed that ATV could induce apoptosis in HeLa cells in a time-dependent manner. The apoptosis rate of ATV-induced HeLa cells was significantly higher than that of the Ad-MOCK control group 48 h after 100 MOI ATV infection [(38.995 ± 4.009)% vs. (14.680 ± 1.174)%; $P<0.01$] (Fig. 2a), and the apoptotic rates at 24, 48 and 72 h were (23.800 ± 2.772)%, (38.995 ± 4.009)% and (45.315 ± 5.013)% (Fig. 2b), respectively. With an increased treatment time, the apoptotic rate peaked at 72 h.

ATV affects the cell cycle

HeLa cells were used to analyze the effect of ATV on the cell cycle distribution by flow cytometry using propidium iodide staining (Fig. 2c). The flow cytometry results showed that there was a considerably greater proportion of cells in the S phase associated with prolonged ATV treatment; however, there was no significant change in the number of cells in the G1 and G2 phases. S phase was extended and cell cycle arrest peaked at 48 h, at significantly higher levels than that observed in the Ad-MOCK group [(58.490 ± 2.447) vs. (43.235 ± 4.419)%; $P<0.05$; Fig. 2d). These findings indicate that the arrest of the cell cycle in S phase following infection with ATV delayed the completion of

the cell cycle, apoptosis and autophagy. Thus, ATV may be involved in cell cycle arrest and thereby impact the proliferation of HeLa cells.

ATV induced changes in the level of protein expression involved in the autophagy of HeLa cells

Following the treatment of HeLa cells with 100 MOI ATV, the cell lysates were subjected to western blotting to monitor the level of LC3-II, p62 and mTOR protein expression (Fig. 3a,b). To examine whether ATV induction and subsequent increases in LC3 are related to the occurrence of autophagy, we analyzed the conversion of nonlipidated LC3-I to lipidated LC3-II as a common marker of autophagic activity. The level of LC3 protein expression gradually increased at 6 and 12 h, peaking at 12 h, and subsequently decreasing to its lowest levels at 24 h compared with the Ad-MOCK group. In the autophagic pathway, the level of p62 protein expression was similar to that of LC3 and reached its lowest level of expression at 24 h. To confirm that the increase in LC3-II reflected an upregulation of functional autophagic degradation, autophagic flux was also analyzed based on the level of p62 (also known as SQSTM1). Beclin-1 exhibited a similar trend as LC3, whereas the level of mTOR protein expression gradually decreased with prolonged treatment time. The western blot results indicated that ATV promoted the early autophagy of HeLa cells.

The level of LC3 and Beclin-1 mRNA expression appeared to exhibit different changes by quantitative real-time PCR

We next investigated whether ATV treatment affected the expression of autophagy-related genes using quantitative real-time PCR. As shown in Fig. 4, the ratio of LC3 (Fig. 3c) and Beclin-1 (Fig. 3d) was significantly elevated at 12 h following treatment with ATV at a concentration of 100 MOI compared with that of the controls. After treating HeLa cells for 6, 12, 24 and 48 h, the level of LC3B and Beclin-1 mRNA expression peaked at 12 h

Fig. 3

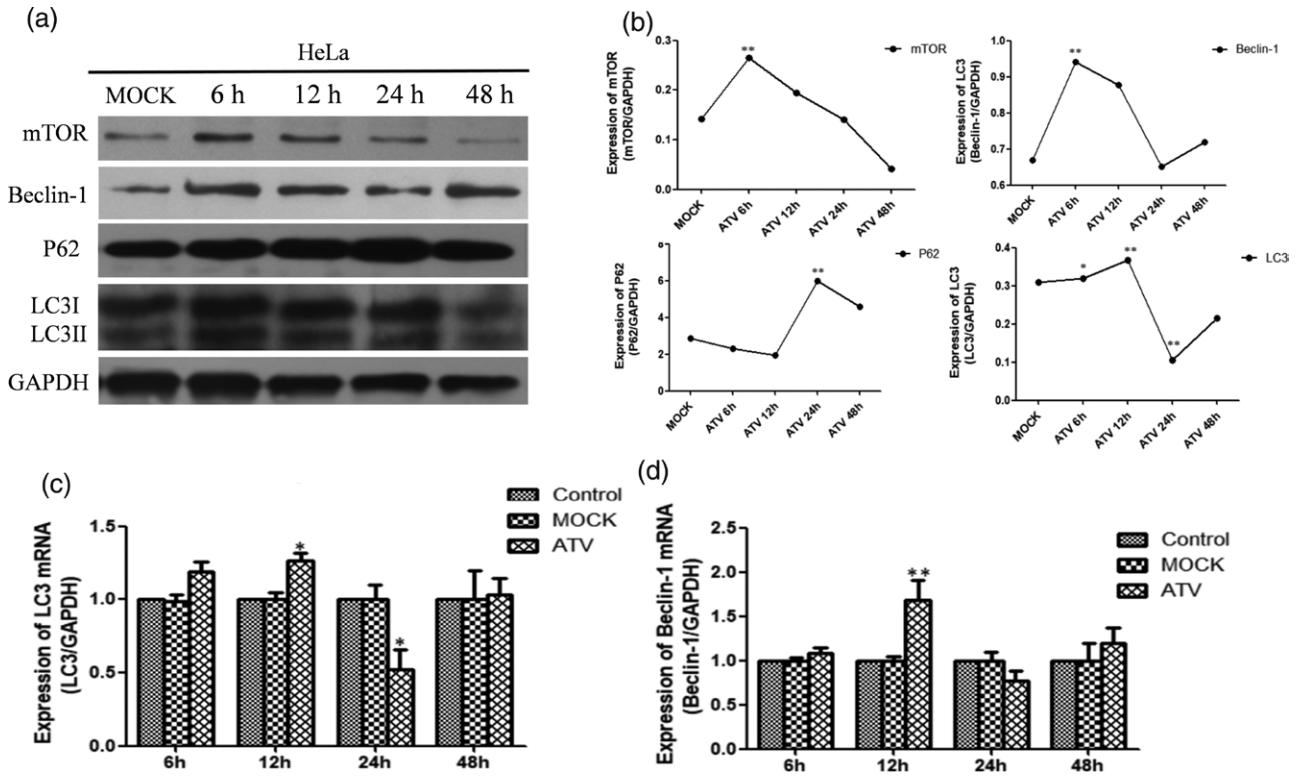

Western blot and real-time PCR analysis, the changes of related proteins and mRNA after ATV-induced autophagy in HeLa cells. Lysates were resolved, and the expression of various components of HeLa cells was analyzed by western blot (a and b). The results show the expression of LC3-I (16 kDa) and LC3-II (14 kDa) in HeLa, p62 (62 kDa) and mTOR (208 kDa) in the cell cultures treated with ATV. Each protein was individually normalized to GAPDH expression. **Significantly different at $P<0.01$ compared to the Ad-MOCK-treated cells (control). Cervical cancer cells were treated with 100 MOI ATV for 6–48 h. After treatment, total RNA was extracted and cDNA was reverse-transcribed from mRNA for real-time PCR of LC3 (c) and Beclin-1 (d). Experiments were performed in triplicate and the data are expressed as the mean ± *SE*. * $P<0.05$ compared with the Ad-MOCK (control) group. GAPDH, glyceraldehyde-3-phosphate dehydrogenase; HeLa, human cervical cancer cell line; MOCK, Oncolytic adenovirus empty vector; MOI, multiplicity of infection; mTOR, mammalian target of rapamycin.

Fig. 4

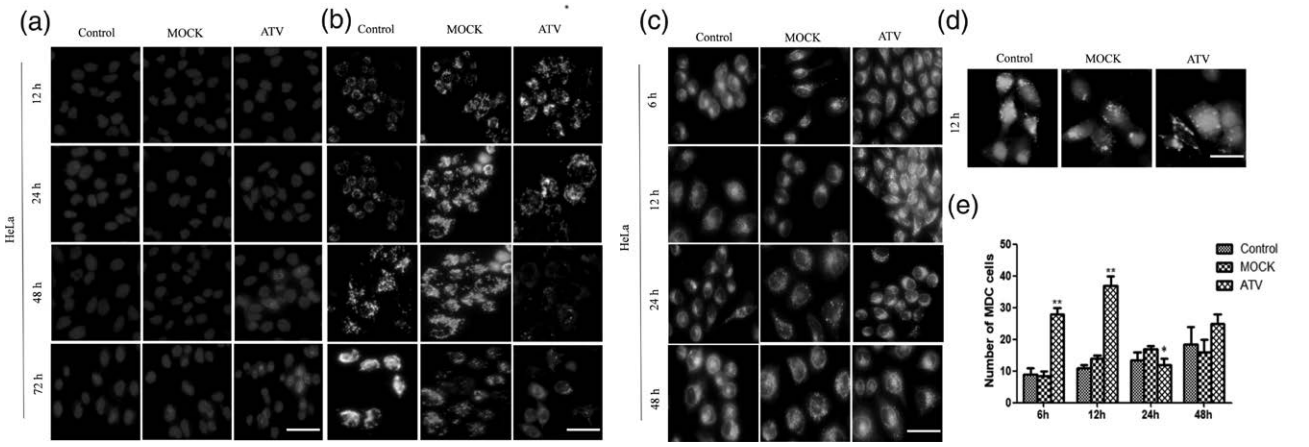

Changes in the degree of apoptosis and autophagy in each group after treatment. Nuclei were stained with Hoechst staining (a; magnification: 400×), and photographed under a fluorescence microscope (Olympus, Japan). Mitochondrial membrane potential monitored using JC-1 solution (b; magnification: 400×). Scale bar: 100 μm. Photomicrograph of HeLa cells treated with 100 MOI ATV and stained with monodansylcadaverine (MDC). A number of massive vacuoles with acidic contents and the accumulation of autolysosomes in HeLa cells (c and e; magnification: 400×). Data were presented as the mean ± SE. The values were statistically significant for * $p < 0.05$ and ** $P < 0.01$, compared with that of the Ad-MOCK control. GFP-LC3 and acidic vesicular organelles expressed in HeLa cells were measured by fluorescence microscopy following treatment with ATV (d). Scale bars: 100 μm. HeLa, human cervical cancer cell line.

and decreased significantly at 24 h, indicating that ATV could regulate autophagy.

Hoechst and JC-1 staining detected ATV-induced HeLa cell apoptosis

Hoechst 33342 is a noninlaid fluorescent dye that binds to DNA in a small groove in the region of the DNA poly adenine thymine sequence in living cells. As a DNA probe, the dye can be taken up by living or fixed cells to stain the nucleus, appearing as bright blue fluorescence. HeLa cells infected with ATV for 12, 24, 48 and 72 h emitted blue fluorescence in the nucleus. Chromatin condensation and nuclear fragmentation were observed in the ATV group (Fig. 4a), indicating that the cells exhibited different degrees of apoptosis. The number of apoptotic cells was determined and the apoptotic rate was 72 > 48 > 24 > 12 h. JC-1 is a fluorescent probe used to detect mitochondrial membrane potential $\Delta\Psi m$. The decline of mitochondrial membrane potential is a significant event in the early stages of apoptosis. After 100 MOI ATV treatment, JC-1 was morphologically transformed from aggregates to JC-1 monomers, in which red fluorescence decreased and green fluorescence increased with the prolongation of ATV infection time (Fig. 4b). The apoptotic effect of HeLa cells was gradually enhanced following ATV treatment, whereas treatment with Ad-Mock did not have a significant effect.

ATV-induced autophagy was observed via monodansylcadaverine staining and transient GFP-LC3 transfection was detected

To investigate the level of HeLa cell autophagy, a monodansylcadaverine staining analysis was implemented, which specifically stains autophagosomes. The perinuclear region of HeLa cells under a fluorescence microscope was observed to be positively stained and exhibit a punctate structure. The number of autophagosomes gradually increased with the prolongation of ATV treatment. Punctate structure aggregation of monodansylcadaverine fluorescence in the proportion of cells increased significantly at 12 h [(37.000.243) vs. (14.000.414); $P < 0.01$] in 100 cells from each group, compared with the Ad-MOCK control group at the same time, indicating an enhanced level of autophagy in HeLa cells. The number of autophagosomes decreased at 24 h [(12.000 ± 2.828) vs. (17.000 ± 1.414); $P < 0.01$; Fig. 4c], which indicated that the form of cell death may be transferred from autophagy to apoptosis, inhibiting autophagy and resulting in a decreased number of autophagosomes. Together, when performing a GFP-LC3 transfection for 12 h (Fig. 4d), the GFP-LC3 fluorescent fusion protein expressed on the cell surface was higher in the ATV-treated group compared to that of the Ad-MOCK group. Moreover, ATV treatment induced further significant formation and accumulation of LC3-GFP puncta compared to Ad-MOCK treatment.

Effect of LC3 expression induced by ATV

The autophagy pathway begins with the formation of the autophagosome, in which organelles or long-lived proteins are phagocytosed followed by maturation into single-membrane autophagosomes which fuse with lysosomes to form 'autolysosomes'. To further determine whether ATV induces autophagy in HeLa cells, we assessed the expression and distribution of LC3-II, a hallmark of autophagy present in the autophagosomal membrane. Moreover, immunofluorescence staining revealed that ATV-treated HeLa cells accumulated

Fig. 5

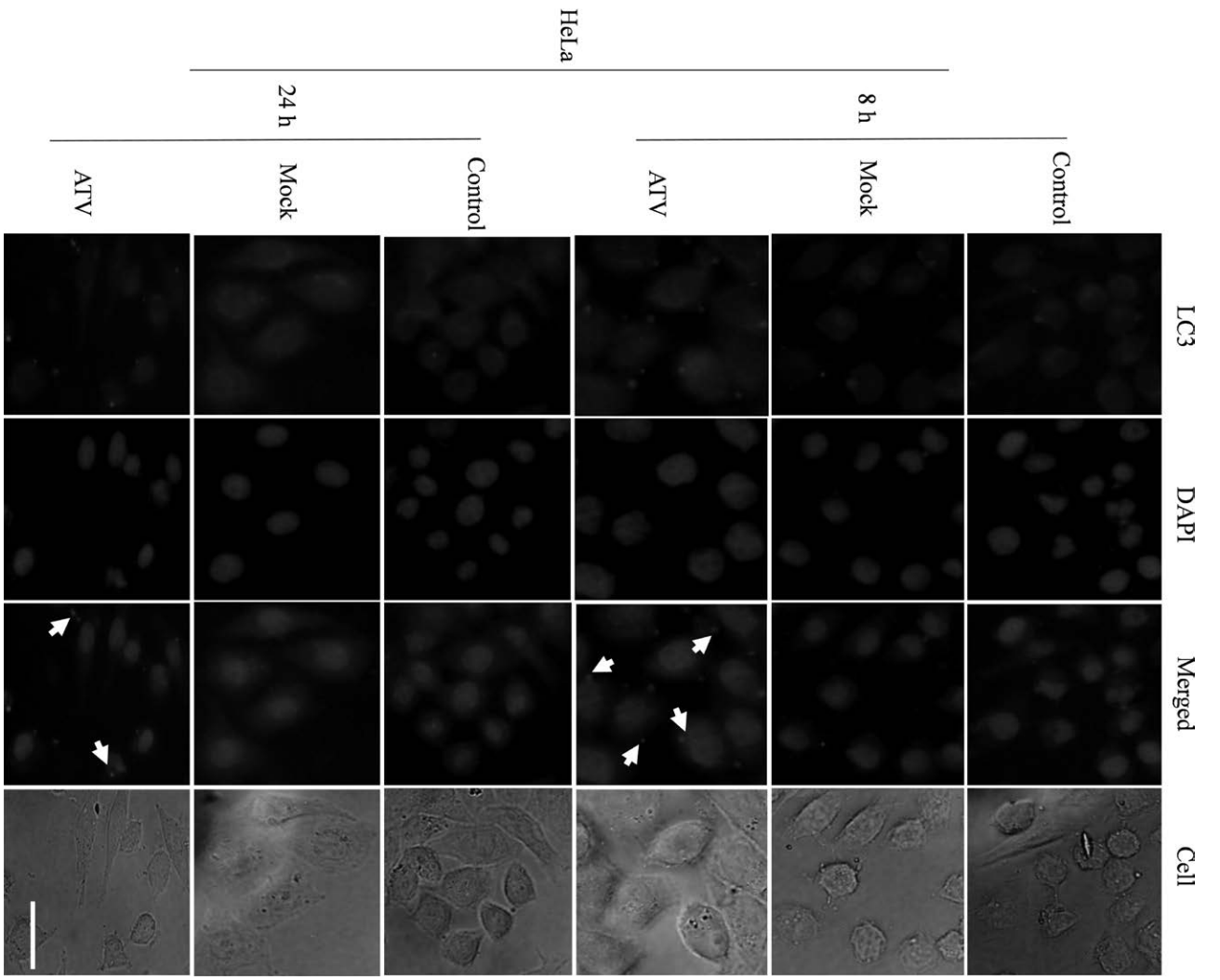

ATV-induced autophagy in HeLa cells and effects of ATV on the expression of autophagy regulatory proteins. Cells were fixed and immunostained with anti-LC3-II antibody (red, magnification: 400×), and the cell nuclei were counterstained with DAPI (blue, magnification: 400×) reagent. Scale bars: 100 μm. ATV, Ad-Apoptin-hTERT-E1a; HeLa, human cervical cancer cell line.

autophagic vacuoles in the cytoplasm (Fig. 5). The level of LC3 protein expression in ATV (100 MOI)-infected HeLa cells was evaluated at 8 and 24 h. The results indicated that the level of LC3 expression was lower at 24 h compared to 8 h, indicating that the level of autophagy at 8 h was greater than that at 24 h; thus, the level of early autophagy was higher.

Transient silencing of LC3 and Beclin-1 was achieved by RNA interference

The qPCR results showed that the level of LC3 and Beclin-1 protein expression in LC3 and Beclin-1 gene-silenced cells was significantly decreased compared with normal and negative control (NC) HeLa cells. The interference efficiency reached (70.3 ± 4.3) and (72.2 ± 5.7)%, respectively (Fig. 6a,b).

Effect of LC3 and Beclin-1 gene silencing on HeLa cell proliferation and apoptotic rate

The level of WST-1 revealed that the inhibitory effect on cellular proliferation reached a maximum value of LC3-si (43.732 ± 1.732)%, Beclin-1-si (43.869 ± 1.869)% (Fig. 6c,d), which was 2.56 and 2.58 times, respectively, higher than that of the HeLa NC group. In addition, the apoptotic rate decreased at 12 h and peaked at 72 h compared with the NC group (Fig. 6e,f).

Effect of Beclin-1 gene silencing on the level of autophagy in HeLa cells

When the Beclin-1 gene was knocked down in ATV-treated cells, the real-time PCR and western blot results showed that the level of LC3 expression decreased at 6 and 12 h. Similarly, using monodansylcadaverine staining,

Fig. 6

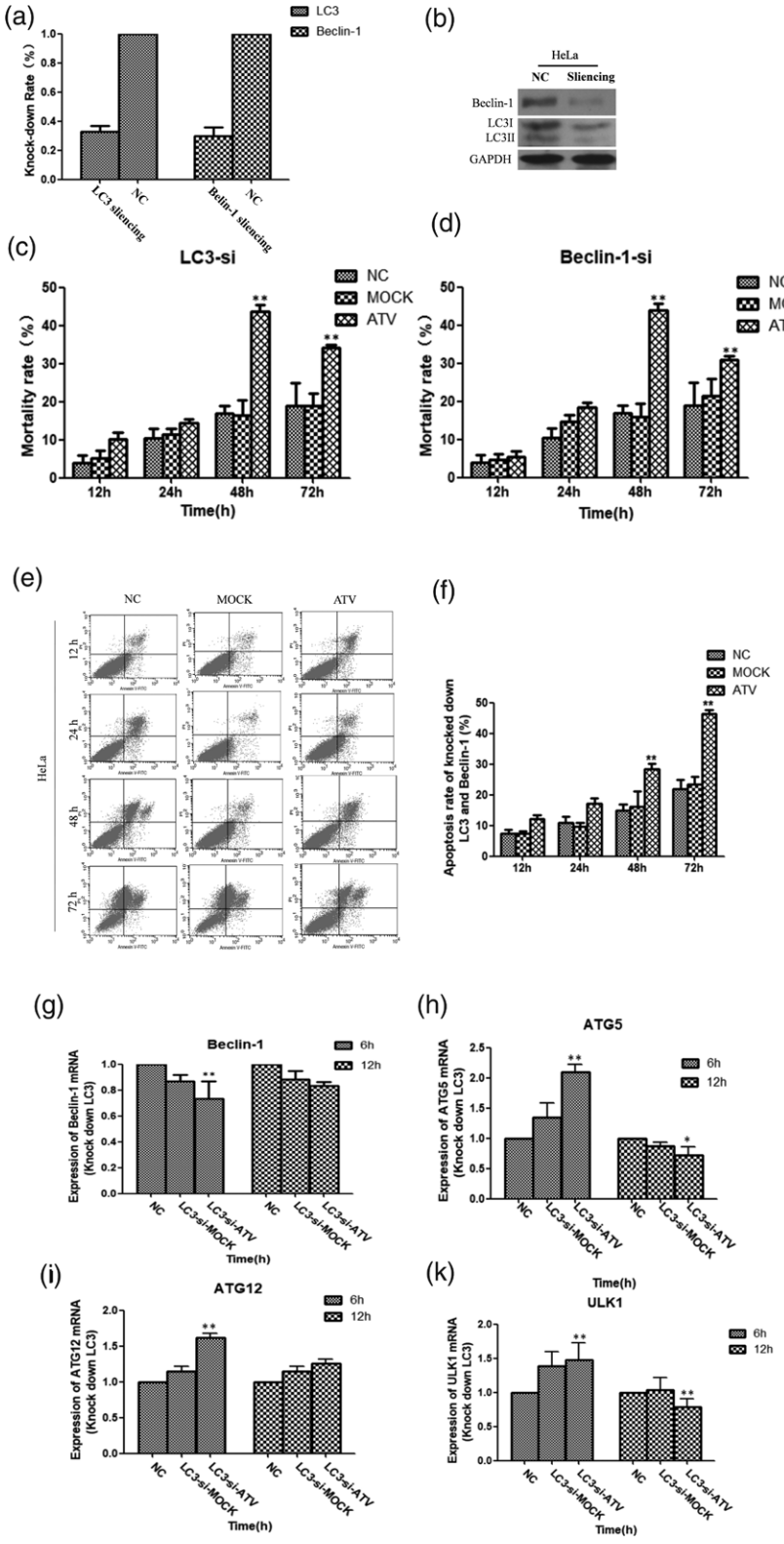

Gene silencing of LC3 and Beclin-1 impacted Hela cell autophagy. siRNA-transfected HeLa cells exhibited high LC3 and Beclin-1 silencing efficiency of (a and b). Moreover, differential effects on cell proliferation and apoptosis were observed compared with the NC group (c–f). After LC3 silencing, Beclin-1, ATG5, ATG12 and ULK1 were upregulated and downregulated at varying degrees for each of the above-mentioned autophagy regulators (g–k). Data are presented as the mean ± SE. Values were statistically significant for * $P<0.05$ and ** $P<0.01$ compared with the negative control group. HeLa, human cervical cancer cell line.

the number of fluorescent spots was found to decrease compared with the NC group, indicating that the number of monodansylcadaverine-traced autophagosomes was reduced.

Effect of LC3 gene silencing on related factors other than autophagy

First, similar to that described above, decreased autophagy was observed following ATV infection in the LC3-si group at 6 and 12 h. We subsequently tested the level of changes made to Beclin-1, ATG5, ATG12 and ULK1 (Fig. 6g–k), which demonstrated that Beclin-1 was reduced and ATG12 increased at 6 and 12 h, whereas ATG5 and ULK1 increased at 6 h and was reduced at 12 h. These findings indicate that LC3-si HeLa cells treated with ATV for 6 h exhibited enhanced autophagic pathways related to ATG12, ATG5 and ULK1.

Discussion

Cervical cancer develops from malignant cells that form in the cervix and is a leading cause of morbidity and mortality in women worldwide [9]. Although the majority of cervical cancer patients have benefited from neoadjuvant chemotherapy together with concurrent chemotherapy and radiotherapy, the survival rate remains poor in cervical cancer patients with relapse or recurrence. Thus, developing novel therapeutic strategies for cancer patients remains a constant requirement. Oncolytic adenoviruses are promising tools for cancer therapeutics due to their ability to be genetically manipulated and exhibit multiple distinct anticancer mechanisms, including direct lysis, apoptosis induction, expression of toxic proteins, autophagy, shutting-down protein synthesis and the induction of antitumoral immunity.

Apoptin is a 13.6 kDa viral protein encoded by the chicken anemia virus VP3 gene and consists of 121 amino acids. Recently, apoptin has attracted widespread attention as both a pioneer in the development of cancer-specific therapeutics, as well as its potential use as an indicator of cellular transformation processes [10]. The hTERT promoter is considered to be a good tumor-specific regulator of oncolytic adenoviruses. The tumor-specific promoter, hTERT, promotes both tumor-specific replication and E1A expression, and several hTERT-driven adenoviruses have been described; [11,12] however, none of these viruses bind promoter elements to a single virus to regulate E1A expression and viral replication. Since hTERT is expressed in more than 90% of cancers [13,14], oncolytic viruses that combine these two characteristics have the potential to induce oncolytic activity in a wide range of human tumors and tumor cell populations. In addition, tumor gene therapy based on oncolytic adenoviruses has been extensively studied in recent preclinical and clinical trials [15]. In our previous studies, we constructed an Ad-hTERT-E1a-Apoptin containing hTERTp and specific antitumor gene apoptin using the RAPAd.I system, which displayed inhibition of tumor-specific growth [16]. Moreover, it was found to induce apoptosis independent of the death receptor pathway in a wide range of transformations and cancer cells and localizes in the nucleus of cancer cells [17–19].

An oncolytic adenovirus (Ad-hTERTp-E1a-Apoptin) has been proven to inhibit cellular growth in various human cancer cells, including SW1116 human colorectal carcinoma cell lines, esophageal cancer EC-109 cells, melanoma cell lines (A375 and B16), the human prostate PC-3 cell line and gastric carcinoma SGC7901 cell line, respectively [20,21].In the present study, we demonstrated that ATV inhibits cellular proliferation, and induces S-cell cycle arrest, mitochondrial membrane potential transformation and nuclear fragmentation in HeLa cervical cancer cells. A WST-1 assay indicated that ATV infection at 100 MOI significantly inhibited the growth of HeLa cells after 48 h and the inhibitory effect of ATV was both dose- and time-dependent. In addition, the Annexin V assay indicated that ATV could suppress the growth of HeLa cells through the induction of apoptosis. Consistent with the WST-1 assay, the Hoechst, JC-1, and Annexin V staining assays demonstrated that ATV displayed the most significant growth-inhibitory effect on HeLa cells and that ATV was significantly stronger than Ad-MOCK. Therefore, RNA interference (RNAi) is a powerful tool for knocking down genes using sequence-specific post-transcriptional targeting [22].

In our study, the apoptosis rate decreased at 12 h and there was no significant difference between the other infection periods and the untransfected groups at the same time points. The first portion of the present study primarily focused on the apoptosis-mediated approach. Moreover, the concept of autophagy provides a novel perspective on the pathogenesis of cervical cancer [23]. The present study found that ATV can both induce apoptosis and regulate the level of autophagy in HeLa cells. Autophagy (type II programmed cell death) is a highly conserved, strictly controlled physiological process that degrades intracellular macromolecules and endogenous substrates using lysosomal pathways LC3 is a homolog of the yeast ATG8 gene in mammalian cells and participates in the formation of autophagosomes [24] In addition, LC3 II is consistently retained on the autophagosome membrane until it fuses with lysosomes, and its content is proportional to the number of autophagic vacuoles [25].

In this study, we first observed an increase in the expression of LC3 II in HeLa cell lines following ATV treatment. It is of particular importance that the level of both LC3 II protein and mRNA expression were upregulated by ATV treatment from 6 to 12 h compared to the control. This finding indicated that the autophagic activity or potential was significantly increased, and the number

of autophagosomes gradually increased. However, the expression of LC3 II was downregulated compared to the control group following ATV infection for 24 h. Thus, it is suspected that the method of cell death may shift from autophagy to apoptosis, thereby inhibiting autophagy and leading to a decrease in the number of autophagosomes. The process by which autophagy is regulated is highly complex, and the key factors associated with its initiation are the related targets of mTOR, including the TOR complex 1 (TORC1) and PI3K [26]. These results suggest that it is possible to regulate cell autophagy by activating the mTOR signal pathway, and the level of mTOR in the ATV-infected group was significantly decreased compared with the control group; moreover, the level of autophagy was substantially increased and cell viability was significantly decreased. The number of autophagosomes and the level of LC3-II expression gradually increased in HeLa cells treated with 100 MOI ATV from 6 to 12 h. Autophagy is an evolutionarily conserved cell survival process that degrades long-lived proteins, damaged organelles, and protein aggregates [27]. The mammalian protein, p62, is selectively degraded by autophagy and can be used as vector receptors or adaptors for the autophagic degradation of ubiquitinated substrates [28]. The enhanced expression of upstream autophagy or a blockade of downstream degradation leads to the aggregation of p62. Finally, p62 is integrated during mature autophagy and degraded in the autophagosomes [29]. The level of p62 is negatively correlated with autophagy [30]. Therefore, LC3 and p62 represent two of the most ubiquitous autophagy-related proteins used to determine autophagy capacity and autophagy. Following ATV induction, the level of p62 peaked at 24 h, whereas autophagy was significantly reduced. In addition, small-interfering RNAs (siRNAs) have been employed to knockdown the expression of cancer-associated genes and exhibit some promise in cancer therapy [28,31,32]. In addition, ATG12 and ATG5 gradually synthesize the ATG5-ATG12 complex, which can form the regulatory system of the LC3 precursor, and provides a preliminary basis for the occurrence of autophagy [33]. ATG12-ATG5, as an autophagic conjugate complex, promotes the elongation of the autophagic membrane and encapsulation and lipoylation of LC3 by combining with ATG12, which regulates autophagosome formation. After the knockdown of LC3 and Beclin-1 in 6 h, to better evaluate autophagy, the results demonstrated that although there was an increasing trend in the level of ATG5 and ATG12 of in ATV-treated HeLa cells, they seemed to have little relationship with LC3 and Beclin-1. Moreover, unc-51-like kinase 1 (ULK1) is a necessary kinase for initiating autophagy under conditions of stress [34,35]. In particular, the ULK1-ATG13-FIP200 complex is activated by adenosine 5'-monophosphate (AMP)-activated protein kinase in response to a low nutritional state [36]. Once activated, ULK1 promotes the formation of the autophagy and autophagy-associated proteins, Beclin-1 and LC3 [37]. Unexpectedly, we found that following ATV treatment, the level of ULK1 displayed a similar trend at 6 h to that of ATG5 and ATG12, in that autophagy-related pathways and the level of autophagy level were enhanced. Therefore, the ATV-induced autophagy in HeLa cells is not entirely dependent on the LC3 and Beclin-1 pathways.

In conclusion, we sought to elucidate the role of ATV on HeLa cells regarding the processes of autophagy and apoptosis. Our results suggest a paralleled event, in which ATV regulates several signaling pathways and targets cellular proliferation by participating in cell cycle arrest and inducing cell death through both autophagy and apoptosis. We provide additional evidence that ATV induces both apoptosis and autophagy, and that the ATG5, ATG12 and ULK1-related pathways are not entirely dependent on LC3 and Beclin-1. Based on these findings, we conclude that ATV may potentially serve as a therapeutic modality for cervical cancer. Therefore, ATV could be beneficial for the treatment of cervical cancer and provide a reasonable treatment strategy for tumor occurrence and development.

Acknowledgements

This work was supported by this research was supported by the Science and Technology Research Project of Jilin Provincial Department of Education [Grant No. JJKH20220873KJ], the Jilin Province Traditional Chinese Medicine Science and Technology Project [Grant No. 2022124], the Major Science and Technology Project for Major Disease Prevention and Control in Jilin Province [Grant No. 20210303002SF] and the Jilin Science and Technology Development Plan Project [Grant No. 20220508075RC].

The datasets used and analyzed during the current study are available from the corresponding author on reasonable request.

Conceived and designed the experiments: S.L., Z.L., S.C., Y.Z., Y.L., X.Y., X.L. and G.Z. All authors read and approved the final article. Conceived and designed the experiments: S.L., Y.L., X.Y., X.L. and G.Z. Performed the experiments: S.L., Z.L., Y.L., Y.Z.. Analyzed the data: S.L., S.C., X.L.. Contributed reagents/materials/analysis tools: S.C., Y.Z., Y.L., X.Y., and X.L.. Wrote the article: S.L. and G.Z.. All authors read and approved the final article.

Conflicts of interest

The research was conducted in the absence of any commercial or financial relationships that could be construed as a potential conflict of interest.

References

1 Castle PE, Einstein MH, Sahasrabuddhe VV. Cervical cancer prevention and control in women living with human immunodeficiency

virus: GLOBOCAN estimates of incidence and mortality worldwide for 36 cancers in 185 countries. *CA: Cancer J Clin* 2021; **71**:505–526.
2 Croswell J, Costello A. Screening for cervical cancer. *Am Fam Physician* 2012; **86**:563–564.
3 Ferlay J, Soerjomataram I, Dikshit R, Eser S, Mathers C, Rebelo M, *et al*. Cancer incidence and mortality worldwide: sources, methods and major patterns in GLOBOCAN 2012. *Int J Cancer* 2015; **136**:E359–E386.
4 Aurelian L. Oncolytic viruses as immunotherapy: progress and remaining challenges. *Onco Targets Ther* 2016; **9**:2627–2637.
5 Lundstrom K. New frontiers in oncolytic viruses: optimizing and selecting for virus strains with improved efficacy. *Biologics* 2018; **12**:43–60.
6 Kaufman HL, Kohlhapp FJ, Zloza A. Oncolytic viruses: a new class of immunotherapy drugs. *Nat Rev Drug Discov* 2015; **14**:642–662.
7 Twumasi-Boateng K, Pettigrew JL, Kwok YYE, Bell JC, Nelson BH. Oncolytic viruses as engineering platforms for combination immunotherapy (vol 18, pg 419, 2018). *Nat Rev Cancer* 2018; **18**:526.
8 Muik A, Stubbert LJ, Jahedi RZ, Geiβ Y, Kimpel J, Dold C, *et al*. Re-engineering vesicular stomatitis virus to abrogate neurotoxicity, circumvent humoral immunity, and enhance oncolytic potency. *Cancer Res* 2014; **50**:S199–S19S.
9 Sullivan SA, Stringer E, Van Le L. A review of gynecologic oncology in the global setting: educating and training the next generation of women's health providers. *Obstetric Gynecol Surv* 2019; **74**:40–49.
10 Park SY, Park C, Park SH, Hong SH, Kim GY, Hong SH, *et al*. Induction of apoptosis by ethanol extract of Evodia rutaecarpa in HeLa human cervical cancer cells via activation of AMP-activated protein kinase. *Biosci Trends* 2017; **10**:467–476.
11 Osaki S, Omori T, Tazawa H, Hasei J, Yamakawa Y, Sasaki T, *et al*. Telomerase-dependent oncolytic adenovirus sensitizes human osteosarcoma cells to chemotherapy through Mcl-1 downregulation. *Cancer Res* 2014; **74**:342–342.
12 Kasi PD, Tamilselvam R, Skalicka-Wozniak K, Nabavi SF, Daglia M, Bishayee A, *et al*. Molecular targets of curcumin for cancer therapy: an updated review. *Tumor Biol* 2016; **37**:13017–13028.
13 Kucharski TJ, Ng TF, Sharon DM, Navid-Azarbaijani P, Tavassoli M, Teodoro JG. Activation of the chicken anemia virus apoptin protein by Chk1/2 phosphorylation is required for apoptotic activity and efficient viral replication. *J Virol* 2016; **90**:9433–9445.
14 Samson A, Scott KJ, Taggart D, West EJ, Wilson E, Nuovo GJ, *et al*. Intravenous delivery of oncolytic reovirus to brain tumor patients immunologically primes for subsequent checkpoint blockade. *Sci Transl Med* 2018; **10**:642–662.
15 Kaufman HL, Kohlhapp FJ, Zloza A. Oncolytic viruses: a new class of immunotherapy drugs (vol 14, pg 642, 2015). *Nat Rev Drug Discovery* 2016; **15**.
16 Nüesch JPF, Bär S, Rommelaere J. Viral proteins killing tumor cells: new weapons in the fight against cancer. *Cancer Biol Ther* 2008; **7**:1374–1376.
17 Bullenkamp J, Tavassoli M. Signalling of apoptin. *Anticancer Genes* 2014; **818**:11–37.
18 Backendorf C, Noteborn MHM. Apoptin towards safe and efficient anticancer therapies. *Anticancer Genes* 2014; **818**:39–59.
19 Castro J, Ribo M, Benito A, Vilanova M. Apoptin, A versatile protein with selective antitumor activity. *Curr Med Chem* 2018; **25**:3540–3559.
20 Yang G, Meng X, Sun L, Hu N, Jiang S, Sheng Y, *et al*. Antitumor effects of a dual cancer-specific oncolytic adenovirus on colorectal cancer in vitro and in vivo. *Exp Ther Med* 2015; **9**:327–334.
21 He D, Sun L, Li C, Hu N, Sheng Y, Chen Z, *et al*. Anti-tumor effects of an oncolytic adenovirus expressing hemagglutinin-neuraminidase of Newcastle disease virus in vitro and in vivo. *Viruses* 2014; **6**:856–874.
22 Li X, Liu Y, Wen Z, Li C, Lu H, Tian M, *et al*. Potent anti-tumor effects of a dual specific oncolytic adenovirus expressing apoptin in vitro and in vivo. *Mol Cancer* 2010; **9**:10.
23 Liu L, Wu W, Zhu G, Liu L, Guan G, Li X, *et al*. Therapeutic efficacy of an hTERT promoter-driven oncolytic adenovirus that expresses apoptin in gastric carcinoma. *Int J Mol Med* 2012; **30**:747–754.
24 Haussecker D, Kay MA. RNA interference. Drugging RNAi. *Science* 2015; **347**:1069–1070.
25 Levy JMM, Towers CG, Thorburn A. Targeting autophagy in cancer. *Nat Rev Cancer* 2017; **17**:528–542.
26 Sharma A, Almasan A. Autophagy as a mechanism of Apo2L/TRAIL resistance. *Cancer Biol Ther* 2018; **19**:755–762.
27 Wu X, Yu J, Yan J, Dai J, Si L, Chi Z, *et al*. PI3K/AKT/mTOR pathway inhibitors inhibit the growth of melanoma cells with mTOR H2189Y mutations in vitro. *Cancer Biol Ther* 2018; **19**:584–589.
28 Lamark T, Svenning S, Johansen T. Regulation of selective autophagy: the p62/SQSTM1 paradigm. *Essays Biochem* 2017; **61**:609–624.
29 Nakano S, Oki M, Kusaka H. The role of p62/SQSTM1 in sporadic inclusion body myositis. *Neuromuscul Disord* 2017; **27**:363–369.
30 Zhang Y, Mun SR, Linares JF, Towers CG, Thorburn A, Diaz-Meco MT, *et al*. Mechanistic insight into the regulation of SQSTM1/p62. *Autophagy* 2019; **15**:735–737.
31 Alegre F, Moragrega A#129;B, Polo M, Marti-Rodrigo A, Esplugues JV, Blas-Garcia A, *et al*. Role of p62/SQSTM1 beyond autophagy: a lesson learned from drug-induced toxicity in vitro. *Br J Pharmacol* 2017; **175**: 440–455.
32 Zhang J, Ding M, Xu K, Mao L, Zheng J. shRNA-armed conditionally replicative adenoviruses: a promising approach for cancer therapy. *Oncotarget* 2016; **7**:29824–29834.
33 Freytag SO, Stricker H, Lu M, Elshaikh M, Aref I, Pradhan D, *et al*. Prospective randomized phase 2 trial of intensity modulated radiation therapy with or without oncolytic adenovirus-mediated cytotoxic gene therapy in intermediate-risk prostate cancer. *Int J Radiat Oncol Biol Phys* 2014; **89**:268–276.
34 Kharaziha P, Panaretakis T. Dynamics of Atg5-Atg12-Atg16L1 aggregation and deaggregation. *Methods Enzymol* 2017; **587**:247–255.
35 Bansal M, Moharir SC, Sailasree SP, Sirohi K, Sudhakar C, Sarathi DP, *et al*. Optineurin promotes autophagosome formation by recruiting the autophagy-related Atg12-5-16L1 complex to phagophores containing the Wipi2 protein. *J Biol Chem* 2018; **293**:132–147.
36 Chen Z-H, Cao J-F, Zhou J-S, Liu H, Che L-Q, Mizumura K, *et al*. Interaction of caveolin-1 with ATG12-ATG5 system suppresses autophagy in lung epithelial cells. *Am J Physiol Lung Cell Mol Physiol* 2014; **306**:L1016–L1025.
37 Mercer TJ, Gubas A, Tooze SA. A molecular perspective of mammalian autophagosome biogenesis. *J Biol Chem* 2018; **293**:5386–5395.